Investigation and modeling of Residence Time Distribution and thermal dissipation in a Dynamic Filtration module

Xiaomin Xie, Christophe Andre, Nicolas Dietrich, Philippe Schmitz, Luc Fillaudeau

Récents Progrès en Génie des Procédés, Numéro 110 - 2017
ISSN: 1775-335X ; ISBN: 978-2-910239-85-5, Ed. SFGP, Paris, France

Investigation and modeling of Residence Time Distribution and thermal dissipation in a Dynamic Filtration module

Xiaomin XIE[a], Christophe ANDRE[b,c,d], Nicolas DIETRICH[a,e], Philippe SCHMITZ[a,e], Luc FILLAUDEAU[a,e]

[a] LISBP, Université de Toulouse, CNRS UMR 5504, INRA UMR792, INSA, Toulouse, France
[b] HEI, Lille, France
[c] INRA, UR638, PIHM, Villeneuve d'Ascq, France
[d] UMET, CNRS-UMR8207, Université de Lille 1, Villeneuve d'Ascq, France
[e] FERMAT, INP Toulouse, CNRS, INSA Toulouse, UPS, France.

Abstract

Bioprocess often associates bioreactor and membrane separation. Bioprocess performances are intrinsically related to the capacity to control and to maintain microbial cells to their optimal activity (integrity, viability and productivity) while industrial operating conditions generate stressful environment or at least no ideal conditions. In present case, high shear rates and Joule effects are generated within a specific dynamic filtration module. Then, Residence Time Distribution (RTD) in a module, named Rotating and Vibrating Filtration (RVF), in which a three-blade impeller rotates between two membranes, was studied in laminar ($Re_{mixing}<1\times10^3$) and turbulent ($Re_{mixing}>3\times10^4$) regimes. In addition, thermal effects of mixing rate under several flow rates and regimes were reported. The magnitude and duration of stressful conditions stand as critical parameters which were quantified and modeled to engineer and to design intensive bioprocess.

Keywords : Dynamic filtration ; Residence time distribution ; Thermal effect ; modeling ; systemic approach

1 Introduction

The principle of Dynamic Filtration (DF) is to generate complex hydrodynamic perturbations (magnitude of velocity and shear stress, time dependent) by mechanical movement (rotation, vibration, oscillation) of membrane or external mechanical forces close to the membrane, to better control membrane fouling. The external force applied to the system can be longitudinal, transverse, torsional, or with a mix of these motions. The DF module used in this experiment, as Fig. 1 shows, is called Rotating and Vibrating Filtration (RVF technology – patent no. FR-97-14825), designed for biological fluid or liquid food. RVF module has been studied in the previous papers [1-3]. This simple mechanical device runs continuously and generates a high shear rate as well as a hydrodynamic perturbation in the small gap, TMP (up to 300 kPa) and rotation frequency can be adjusted to optimize the operating condition. The critical Reynolds numbers was obtained by previous study [1]: laminar ($Re_{mixing}<1\times10^3$) and turbulent ($Re_{mixing}>3\times10^4$).

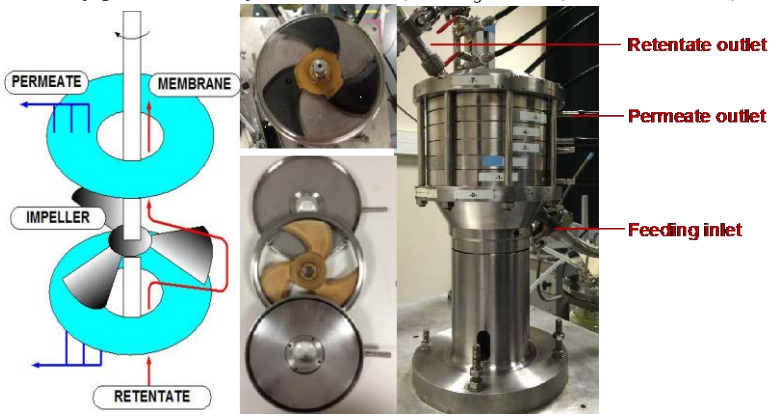

Corresponding author: XIE Xiaomin, E-mail: xxie@insa-toulouse.fr

ISSN: 1775-335X ; ISBN: 978-2-910239-85-5, Ed. SFGP, Paris, France

Fig. 1 Scheme, top view of one filtration cell and global view of Rotating and Vibrating Filtration module.

In this paper, investigation of RTD was performed in a pilot plant with RVF module integrated in a multi-instrumented loop. Our objective were: (1) to study the impact of processing conditions (flowrate, rotation speed) on RTD in an industrial pilot-plant (RVF); (2) to compare through distribution functions the RVF hydrodynamic behaviors in laminar and turbulent regimes; (3) to evaluate the homogeneity within the device and (4) to validate a reactor model to predict RTD. In the first step, trajectory experiments were performed and scrutinized with different process conditions (flowrate, mixing rate) with Newtonian fluids, embracing laminar and turbulent regimes. Experimental data were interpreted thru the sets of moment and centered moments deduced from distribution functions. Their statistical deviation and evolution were discussed as a function of the process parameters. In a second step, a systematic analysis based on experiment data lead to compare and evaluate 4 conventional reactor models. Convolution of inlet distribution x(t) with outlet function y(t) was considered. One model fit with experiments and enable to predict the distribution function, E(t) in RVF module.

2 Theory

2.1 Residence Time Distribution (RTD)

The distribution of these times is called the RTD function of the fluid *E(t)*, or *E*-curve, and represents the fraction of fluid leaving the system at each time [4]. Practically, experimental injection cannot be a perfect and direct signal. In the experiment point of view, normalized signals *x(t)* and *y(t)* were defined for inlet and outlet, presents as Eq.(1). The product of the convolution can be replaced in the Laplace domain by a simple product, where *X(s)*, *Y(s)* and *G(s)* are the Laplace transform of *x(t)*, *y(t)* and *E(t)*, as Eq.(2) presents:

$$y(t) = \int_0^t E(u)x(t\text{-}u)du \text{ and } Y(s) = G(s)X(s) \quad \text{(1) and (2)}$$

Practically, x(t) and y(t) are calculated from experimental signal $C_{in}(t)$ and $C_{out}(t)$ respectively, expressed as Eq. 3, and its cumulative function can be obtained as Eq. 4.

$$E(t) = \frac{C_{out}(t)}{\int_0^\infty C_{out}(t)dt} \text{ and } F(t) = \int_0^\infty E(t)dt \quad \text{(2) and (4)}$$

RTD function can be expressed by moments and centered moments of orders I [5]. The mean residence time, t_s, is characterized by a moment of first order, Γ^1. The holding time, a theoretical value τ, is calculated by the volume of the test system and the feeding flow rate, as Eq.(6) shows. For most of the simple system, t_s and τ must be equal, the closer they are, the closer to the ideality. However, in some complex system, it is not the case. By knowing t_s- τ ratio *k* as Eq.(7) presents, flow behavior can be diagnosed if system has a shortcut of exit or a circuit in the dead zone (volume V_2), effective volume V_1 is defined by t_s.

$$\Gamma^1 = t_s = \int_0^\infty tE(t)dt \text{ and } \tau = \frac{V}{Q_f} \quad \text{(5) and (6)}$$

and

$$k = \frac{t_s}{\tau} = \frac{V_1}{V_{RVF}} \quad (V_1 = t_s \times Q_f, V_{RVF} = V_1 + V_2) \quad \text{(7)}$$

The centered moments of second order, Γ^2, presents the variance σ^2, as Eq. (8) shows, and its corresponding dimensionless term β^2, as Eq. (9) shows. The second centered moment is a very important parameter to describe the width of a distribution, ideal plug flow reactor has $\beta^2 = 0$, $\beta^2 > 0$ indicates an axial dispersion, the smaller the value the narrow the distribution curve and the lower the axial dispersion as well [6].

$$\Gamma^{2'} = \sigma^2 = \int_0^\infty (t\text{-}t_s)^2 E(t)dt = \int_0^\infty t^2 E(t)dt\text{-}t_s{}^2 \text{ and } \beta^2 = \frac{\sigma^2}{t_s^2} \quad \text{(8) and (9)}$$

The centered moments of third order, $\Gamma^{3'}$, presents the skewness, as Eq. (10) shows. It is helpful to determine the symmetry where S=0 indicates a symmetrical distribution, a left-skew distribution for S<0 and a right-skew distribution for S>0.

$$\Gamma^{3'} = S = \int_0^\infty (t\text{-}t_s)^3 E(t)dt \quad (10)$$

The centered moments of forth order, $\Gamma^{4'}$ as Eq. (11) shows, estimates the spread of the RTD, indicates the kurtosis of the distribution function, it describes how heavy-tail (spread) the curve distributes.

$$\Gamma^{4'} = \int_0^\infty (t\text{-}t_s)^4 E(t)dt \quad (11)$$

All moments and centered moments of order can be calculated. However, researchers point out the quality of the signals often leads to non-significant or unreliable results for the moment of higher order.

2.2 Thermal balance

In order to realize thermal balance, power consumption of RVF module was estimated from power consumption curve. The flow is supposed to be incompressible and stationary, and the gravity is neglected. A non-slip condition is imposed on the walls and the inlet speed profile is the same as the outlet profile, then it gives:

$$\Delta P \cdot Q + \iint_A \sum_{j=1}^{3}\sum_{i=1}^{3} \tau_{if} n_i U_j \, ds + \iint_A \sum_{i=1}^{3} (-P) n_i U_i \, ds = \iiint_D \rho \varepsilon_V dv \quad (12)$$

1st term: necessary pump power to drive the fluid in the circulation loop;
2nd term: external viscous forces of by the impeller;
3rd term: external forces of the pressure by the impeller;
4th term: total power dissipation in the field.

Moreover, we assume the uniform temperature at the input and output sections and the heat capacity independent of T, heat dissipation can be simplified by effective power:

$$P_{eff} = \iiint_D \rho \varepsilon_V dv = \rho C_p (T_{inlet}\text{-}T_{outlet}) Q_l \quad (13)$$

3 Materials and Methods: experimental set-up, fluids and operating conditions

Fig. 2 shows the experimental set-up which was implemented with: (1) an open loop configuration and specific inlet and outlet tank, (2) tracer injection unit and (3) conductivity sensors at the inlet and outlet of RVF module.

For experiments in laminar regime, the fluid was stored at room temperature in a 50 L plastic tank (feeding tank) and connected to the RVF inlet, outlet was connected to 50 L plastic tank (collecting tank) for recycling. In turbulent regime, the fluid was not recycled (open loop). Two identical stainless steel straight tubes (diameter 12 mm, length 125 mm, volume 14mL) were used to connect the conductivity sensors with RVF module.

The injection device connected with a mixer was developed to achieve homogenous syringe injections of the tracer. Tracer solutions (100 g/L NaCl) were injected with a 5 mL syringe through a septum. A short injection time (<5s) and a static mesh mixer (Fig. 2b) ensure a homogenous distribution of tracer (close to an ideal pulse injection). Then the tracers were measured by electrical conductivity sensors at the inlet and outlet of the RVF module.

A water soluble and viscous transparent Newtonian fluid (BREOX® Polyalkylene Glycol 75 W 55000, BASF) was used to achieve laminar flow (35% w/w diluted BREOX solution with μ = 0.35 Pa·s, Cp = 3650 J/(kg·°C) and ρ = 1040 kg/m3 at T=20°C), and water was used for the turbulent flow. Mixing Reynolds number can be estimated and validated by previous study; flow regime is confirmed as well.

ISSN: 1775-335X ; ISBN: 978-2-910239-85-5, Ed. SFGP, Paris, France

Power consumption curves enable to identify the flow regimes [1], and experiments were conducted under both laminar (Re_{mixing}<1×10^3) and turbulent (Re_{mixing}>3×10^4). The Residence Time Distribution investigation was restricted to two Newtonian fluids BREOX solution and water for laminar and turbulent flow respectively. (Laminar flow: flowrates Q_f ranging from 25 to 100 L/h, and mixing rate N from 0 to 25 Hz; Turbulent flow: Q_f ranging from 50 to 300 L/h, and mixing rate N from 0 to 50 Hz.) During all the measurements, the fluid properties and operating parameters were stable, inlet fluid temperature is at 13 - 15°C (+/- 0.1°C) under turbulent flow (tap water) and at 17 - 22°C (+/- 0.14°C) under laminar flow. Data acquisition rate were 0.17 to 0.2s.

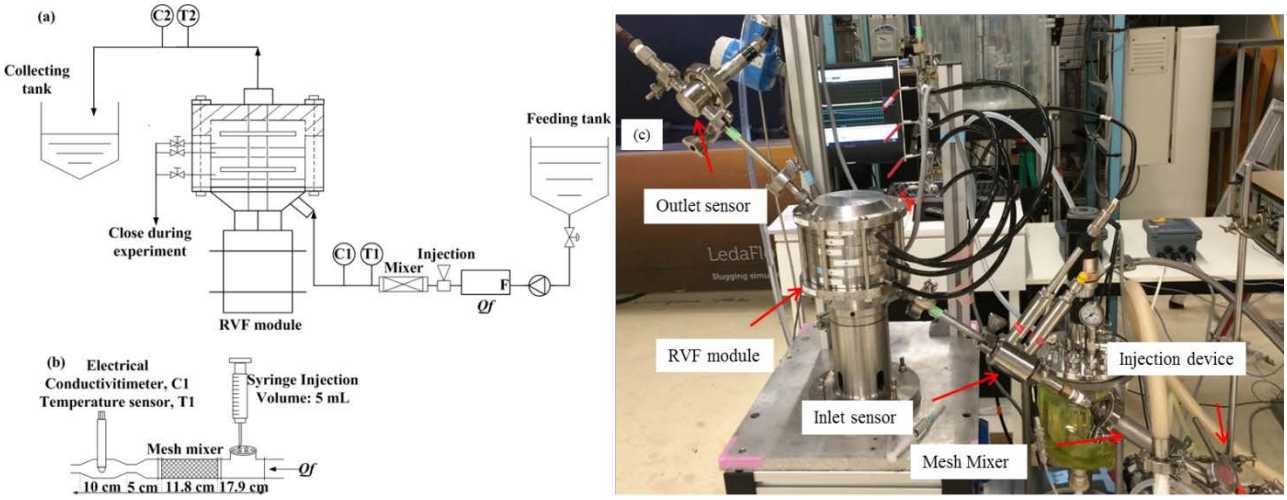

Fig. 2 Experimental setup and injection device (a) schematic of experimental setup, C1, C2: Electrical conductivity sensors; (b) Injection device; (c) Photo of experimental setup.

4 Results and discussion

4.1 Thermal balance

Thermal balance (viscous dissipation) is highly correlated to mixing power. As a result, temperature increases significantly with the increase of mixing rate and the reduction of flow-rate. For example, as Fig. 3 shows, in laminar flow (BREOX solution) with Q_f=25 L/h and N=25 Hz, temperature increased 11°C; in turbulent flow (water), with Q_f=50 L/h and N=50 Hz, temperature increased 9°C.

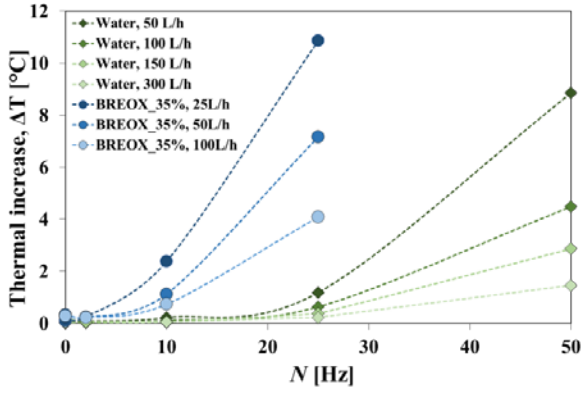

Fig. 3 Temperature variation of the test fluid with different mixing rate

In agreement with theory (Eq.12 and 13), Fig. 4 shows the variation of heat dissipation and efficient power consumption [W] under different mixing rate in both laminar and turbulent regimes. Due to its higher viscous force (2nd term of Eq.12) in laminar regime, temperature (as well as heat dissipated) increases faster than in turbulent regime (for example Q_f =50 and 100 L/h). As indicates with the solid curves, the effective power consumption is estimated from a power consumption curve model in previous

research [1], $Np = \left(B^{\frac{1}{n}} + \left(\frac{Kp}{Re_{mixing}} \right)^{\frac{1}{n}} \right)^{n} \cong \frac{Kp}{Re_{mixing}}$, (equation (14)) where n=2, B=0.10, Kp=520, by knowing mixing Reynolds.

In a bioprocess context, maintaining ideal culture temperatures is vital for optimal cell growth. The selected temperature highly depends on the nature of the cells to be cultured. In addition to culturing, there are temperature considerations when it comes to storing cells. The maximum temperature for growth depends on the thermal sensitivity of secondary and tertiary structures of proteins and nucleic acids. The minimum temperature depends mainly on the freezing temperature. Different physiological groups of microorganisms adapt to different temperature. Psychrophiles have optimal temperatures for growth below 15°C. Mesophilic have optimal growth temperatures in the range between 20 and 40 °C. thermophiles grow best between 50 and 70°C. There are known thermoextremophyles growing at temperature higher than 70°C [7]. For example, prokaryote cells E. coli's optimal temperature to live in is around 37°C and Streptomyces griseus is at 25 to 35C; for eukaryote cell Saccharomyces cerevisiae is 31 to 35°C and Saccharomyces uvarum around 36 to 30°C [8].Considering a temperature increase limited to 4°C (compatible with cell culture), restricted operating conditions (minimum flowrate and maximum mixing rate) can be estimated from Eq.(13 and 14) including thermal balance and power consumption.

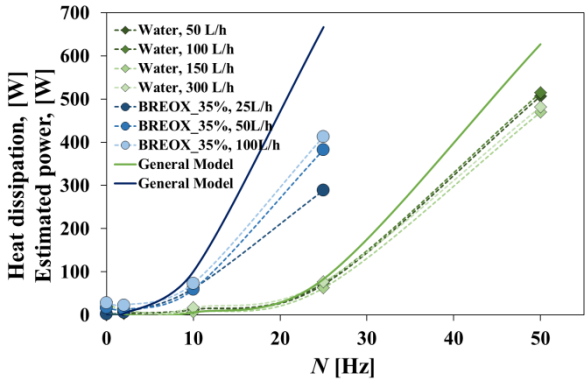

Fig. 4 Heat dissipation [W] and estimated power consumption [W] as a function of mixing rate under laminar and turbulent regimes.

4.2 Residence Time Distribution (RTD)

In this part, an analytical study concerning experimental observations is firstly reported and moments are discussed. Then reactor modeling through systemic approach is proposed.

4.2.1 Analytical studies: discussion of moments

Analytical results will be discussed on moments and centered moments. Following Thereska (1998) [9], experimental inlet and outlet RTD signals, x(t) and y(t) are formulated. The measured conductivity values were converted into concentration values for a reference temperature. The concentration profiles were obtained as a function of time in laminar and turbulent regimes respectively.

- **Moment of 1st order (mean residence time)**

Moment of first order Γ^1 represents the mean residence time t_s in the system, as expressed by Eq. (5). These mean residence time, ts, will be compared to the holding, τ.

ISSN: 1775-335X ; ISBN: 978-2-910239-85-5, Ed. SFGP, Paris, France

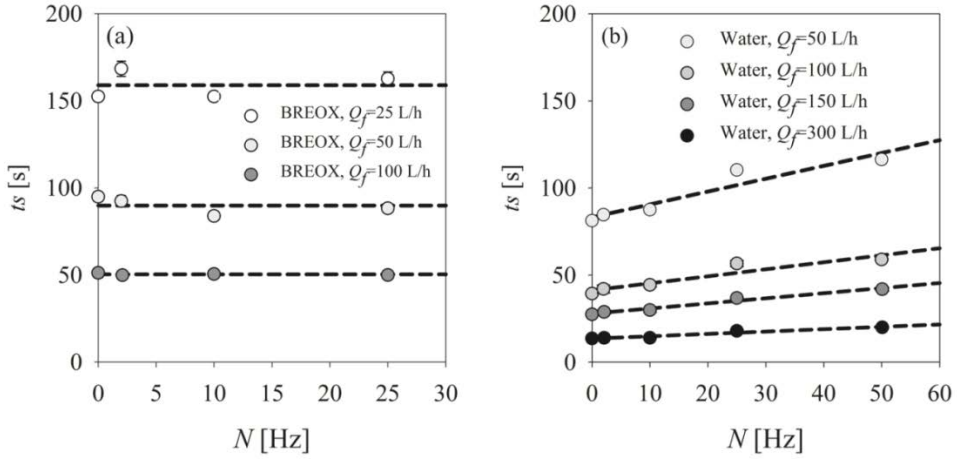

Fig. 5 Mean residence time t_s as a function of rotation speed N for (a) laminar flow regime, operating condition: BREOX solution μ=0.35 Pa·s, Q=25, 50, 100 L/h, N=0, 2, 10, 25 Hz; and for (b) turbulent flow regime, operating condition: water, Q=50, 100, 150, 300 L/h, N=0, 2, 10, 25, 50 Hz

Fig. 5 a and b plot t_s as a function of N in laminar and turbulent regimes. As expected, t_s decrease as Q_f increases.

In laminar flow, t_s remain constant at a given Q_f, whatever the N is. The product $t_s \cdot Q_f$ indicates that the effective volume: for Q_f= 25L/h, V_1= 1.12 L ± 0.06; for Q_f =50L/h, V_1=1.27 L ± 0.07; for Q_f =100 L/h, V_1=1.34 L ± 0.02. Effective volume is only flow rate dependent, the mixing rate do not seem to have impact.

In turbulent flow, t_s increases linearly as a function of N at a given Q_f. In this case, the effective volume is only mixing rate dependent whereas flow rate does not have any effect. V_1 can be described by a semi-empirical relation with Q_f and N considering the mean residence time, *ts.* :

$$t_s = \alpha N + \tau_0, (\text{or } V_1 = \alpha N + V_0) \tag{14}$$

where α (or τ_t) is as function of $1/Q_f$ ($R^2 \geq 99\%$), t_s and V_1 can be generally described by Q_f and N, with an initial volume of 1.15L, which is close to the effective volume V_1 in laminar flow.

$$V_1 = t_s \cdot Q_f = \alpha N + V_0 = 0.0106 \cdot N + 1.15 \tag{15}$$

It is noticeable that effective volume will just depend on mixing rate in turbulent regime.

Mean residence time, t_s reflects the real movement of the tracers in RVF module (including shortcut, bypass, dead-zone may if existing), while τ represents the holding time based on the assumption that tracer molecules ideally move all volume of RVF module. Therefore, ratios, t_s / τ or V_1/V_{RVF}, can be one of the important parameters to diagnose efficient volume. The closer are the ratio to 1, the closer the system feet to ideal case. As it is illustrated inFig.6, in laminar (Re_{mixing}<1×10^3), used volume remains constant as a function of mixing Reynolds number at each flowrate. The main contributor that improves the used ratio is the increase of the flowrate Q_f, rotation speed N doesn't drive the flow to reach all over the system. To explain, at first, N was limited to 0-25 Hz which might be not high enough to drive the fluid. Besides, it probably due to that laminar flow is very stable as widely known, the mixing effect in this kind of flow is poor. However, in turbulent regime (Re_{mixing}>3×10^4), generally, initial used ratio is almost the same value as laminar flow at low rotation speed, and it has a rapid growth of used ratio as the increase of rotation speed. Moreover, flowrate in turbulent flow somehow affects the used ratio as the opposite way as in laminar flow: in laminar flow, used ratio increase from 0.76 to 0.90 with the increase of flowrate from 25 to 100 L/h; in turbulent flow, apparently, flow with lower flowrate seems has higher used ratio. Special attention should be paid for the used ratio which is higher than 1, the reason to explain this behavior is that the tracer molecule goes into the dead-zone and it is slowly mixed out of the system. Overall, these observations lead to the fact that, in laminar flow, mixing driving force is mainly the Q_f;

while in turbulent flow, mixing driving force is largely improve by the rotation speed, and lower Q_f may help to have a better mixing.

- **Centered moment of 2nd order, (reduced variances, β^2)**

In Fig.7 experimental reduced variance, β^2 is analysed versus mixing Reynolds. There is a significant decrease in reduced variance under both the laminar and turbulent regime. It is noticeable that with higher flowrate the system seems closer to a perfect mixer, and with higher Re_{mixing} it has lower value which may tend to more similar as a plug flow reactor. Considering Q_f= 50 and 100 L/h in both flow regime, two logarithmic regressions are plotted, which denotes that β^2 and mixing effect (Re_{mixing}) are somehow related.

- **Centered moment of 3rd and 4th orders**

Centered moment of 3rd and 4th order estimates the skewness and the spreading of RTD curves. In our case, Γ^3 and Γ^4 of all the experiments have positive values, indicating that, generally, RTD curves in RVF module is right-skewed and has a tail spreading. Mixing effect appears as the predominant effectors compared to flow rate, and values are signiciatly higher in laminar that in turbulent laminar regimes. For instance, Γ^3 and Γ^4 are equal to 4.4×10^6 ($\pm1.5\times10^6$), 8.8×10^9 ($\pm2.1\times10^9$) (operating condition: BREOX, Q_f=25 L/h, N=25 Hz) and 1.9×10^5 ($\pm1.3\times10^4$), 6.8×10^8 ($\pm6.4\times10^7$) (operating condition: water, Q_f=50 L/h, N=50 Hz) for laminar and turbulent regimes respectively. However, further interpretation is limited by these poorly significant and reliable calculations

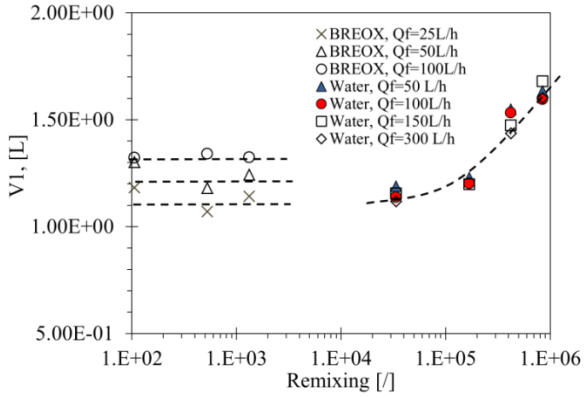

Fig. 6 Used volume V1 as a function of mixing Reynolds number. Laminar flow regime Re_{mixing} <1×10³: operating condition: BREOX solution μ=0.35 Pa·s, Qf=25, 50, 100 L/h, N=0, 2, 10, 25 Hz; Turbulent flow Re_{mixing} >3×10⁴ operating condition: water, Qf=50, 100, 150, 300 L/h, N=0, 2, 10, 25, 50 Hz

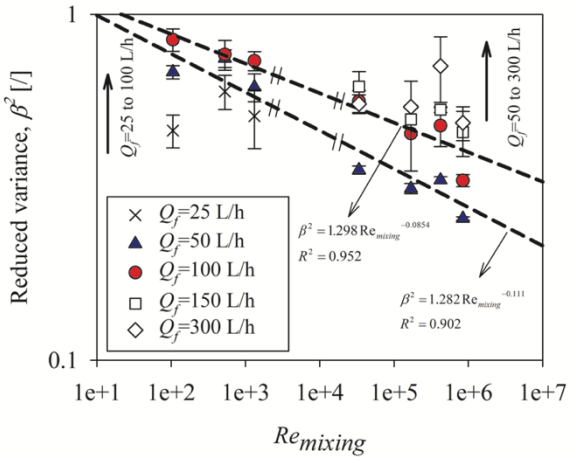

Fig. 7 Reduced variance β^2 as a function of mixing Reynolds number. Laminar flow regime: Re_{mixing}<1×10³, operating condition: BREOX solution μ=0.35 Pa·s, Q=25, 50, 100 L/h, N=0, 2, 10, 25 Hz; Turbulent flow regime: Re_{mixing}>3×10⁴ operating condition: water, Q=50, 100, 150, 300 L/h, N=0, 2, 10, 25, 50 Hz

4.2.2 Systemic analysis and modeling of RTD

After the analytical studies of RTD, in the second step, the hydrodynamic behaviors of the RVF module was describe by a systematic analysis of the RTD modeling signals, by using DTS Progepi v4.2 (Leckerc et al., 1995). Our objective is to model and to establish an analytical solution of RTD functions considering the complexity of RVF module.

4.2.2.1 Proposal of reactor models

4 models were proposed to fit the outlet function *y(t)* of RVF module in order to obtain a better agreement. Inlet function *x(t)* was taken into account due to the imperfect injection. The objective of this modeling is to find the analytical solution to represent the complex designed RVF module. To this aim, conventional models, such as Plug Flow reactor, continuous flow stirred-tank reactor (CSTR) or their

ISSN: 1775-335X ; ISBN: 978-2-910239-85-5, Ed. SFGP, Paris, France

combine forms PFR+(J) CSTR, are proposed, with the ideal PF reactor equivalent to the real tubes before and after the RVF module, describes as Fig. 8 shows:

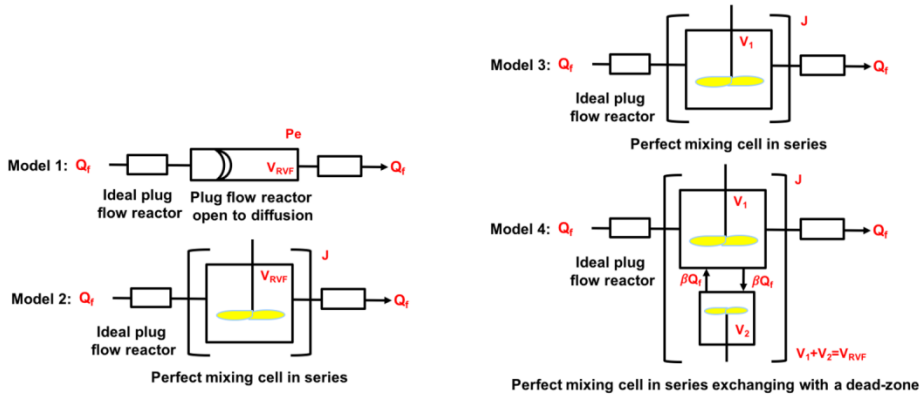

Fig. 8 Proposed models equivalent to RVF model, with the ideal plug flow reactor equivalent to the real tubes before and after. Model 1: Plug flow reactor open to diffusion by imposing V_{RVF}; Model 2:perfect mixing cell in series by imposing the entire volume of RVF module; Model 3: perfect mixing cell in series by imposing the used volume V_1 of RVF module; Model 4: perfect mixing cell in series exchanging with a dead-zone V_2, by imposing V_1 to the mixing cell.

Model 1: PFR+PFR reactor open to diffusion by imposing VRVF and adjusting Peclet number PeL, shown in Fig. 8a. Model 1 considered the association in serie of 2 PF reactor. The first one behaves as an ideal plug (pure delay) whereas the 2nd one is open to diffusion and its volume is imposed to VRVF. Consequently, this model exhibit only 1 degree of freedom by adjusting Peclet number, PeL. RTD function is described by an analytical solution (Eq.17). The current model considers mass transport in the axial direction as a diffusion-like process (analogous to Fick's diffusion law) in terms of an effective longitudinal diffusivity, Dax (axial dispersion coefficient), which is superimposed on the plug flow. The concentration C, of the tracer injected uniformly over the cross-section at the inlet of the system, is given as a function of time t, and the streamwise coordinate z, by Eq.(16). The axial dispersion coefficient is assumed to be independent of the concentration and the position. The first assumption is usually verified if molecular diffusion can be neglected, and the second can be used when a fully developed flow is obtained at the inlet and outlet of the process.

$$\frac{\partial C}{\partial t} = D_{ax}\frac{\partial^2 C}{\partial z^2} - U\frac{\partial C}{\partial z} \tag{16}$$

The transfer function G, of the plug flow with the axial dispersion model, when dispersion extends from before the inlet detector to after the outlet detector. This choice for the boundary conditions (called "open-open") leads to the following expression:

$$E(t) = \frac{1}{2}\left(\frac{Pe_L}{\pi\tau t}\right)^{1/2} exp\left(-\frac{Pe_L(\tau - t)^2}{4\tau t}\right), where\ \tau = \frac{V_{RVF}}{Q_f} \tag{17}$$

$$\text{with } \frac{t_s}{\tau} = 1 + \frac{2}{Pe_l}, \quad \beta^2 = \frac{\sigma^2}{t_s{}^2} = \frac{2}{Pe_L} + \frac{8}{Pe_L{}^2} \text{ and } Pe_L = \frac{LU}{D_{ax}}, \tag{18) and (19)}$$

PeL is calculated from the pipe length and is a dimensionless measure of the axial dispersion, Dax. The DPF model is supposed to yield the best agreement between numerical and experimental results. Furthermore, it has the advantage of necessitating the estimation of only one parameter, i.e., the Peclet number, PeL, Eq. (19).

Model 2: PFR+(J) CSTR model by imposing V_{RVF} and this model exhibit only 1 degree of freedom adjusting the number of mixing cell *J*. In order to obtain a better agreement, a second model defined by a cascade of a plug reactor (τ_p) in series with 2 CSTR (τ_{cs}) was investigated (Fig. 8b). This model was chosen because it is simple and correlates closely to the physical structure of the process. However, other models can also be used as reported by Ham and Platzer. The corresponding expressions for the transfer function, *G(s)* and *E(t)* are formulated by Eq.(20) and Eq.(21):

$$G(s) = \frac{exp(-s\tau_p)}{\left(1+\left(\frac{s\tau_{cs}}{2}\right)\right)^J}, where\ \tau = \frac{V_{RVF}}{Q_f} \quad (20)$$

$$E(t) = H(t-\tau_p)\left(\frac{J}{\tau_{cs}}\right)^2 (t-\tau_p) exp\left(\frac{-J(t-\tau_p)}{\tau_{cs}}\right), \text{ with } \tau=\frac{V_1}{Q_f} \quad (21)$$

The main advantage of this simple model is that only one parameter a, is used, which is the plug reactor contribution, in terms of residence time, Eq. (22). Van Laar's equation leads to a simple relationship between a and β^2, Eq. (26):

$$a = \frac{\tau_p}{\tau_p+\tau_{cs}} \text{ and } \beta^2 = \frac{(1-a)^2}{2} \quad (22) \text{ and } (23)$$

Model 3: PFR+(J) CSTR model. Instead of imposing the total volume of RVF module, this model is based on imposing V_1 (value from experiments) to the mixing cells volume and it exhibits only 1 degree of freedom by adjusting J, governing equation presents as Eq. (21), with $\tau=\frac{V_1}{Q_f}$;

Model 4: PFR+(J) CSTR model exchanging with a dead-zone. Considering a dead-zone may exist in the system, this model taking the exchanging flow by imposing V_1 to the mixing cell (with $\tau = \frac{V_1}{Q_f}\tau=\frac{V_1}{Q_f}$) and it exhibits 2 degree of freedom by adjusting J and β (the ratio between the exchanging flowrate in the dead zone and the feeding flowrate).

4.2.2.2 Model adjustment and comparison

Even if inlet signals can be neglected, we observed injection may slightly differed from ideal Dirac functions, especially in laminar regime. Consequently, to fit the experimental functions, *y(t), the* inlet functions, *x(t)* were considered with all models to simulate *E(t)*. The function *E(t)* was obtained for all the experiment.

Special attention should be paid to the result of Model 4, it was proved that average value of β is inferior to 2%. It means that only 2% of the main flow has exchange with the dead-zone, which can be neglected. In this case, Model 4 is equivalent to Model 3. Therefore, Fig. 9 plots the modeling curve *y(t)'* of Model 1, Model 2 and Model 3 fitting with the experimental data *y(t)*. Result shows that, to fit the experimental data of laminar flow, Model 1 has an overlapping coefficient OVL=0.66, Model 2 OVL=0.77 and Model 3 OVL= 0.89; whereas in turbulent flow, Model 1 OVL=0.66, Model 2 OVL=0.87 and Model 3 OVL= 0.98. Significantly, Model 3 is preferred in both laminar and turbulent flow. The adjustable parameter *J* is calculated and gave an average value of 2.5±0.6. To conclude, PFR+(J) CSTR model by imposing effective volume V_1 *and* J=2.5±0.6 is chosen to describe flow behavior in RVF module.

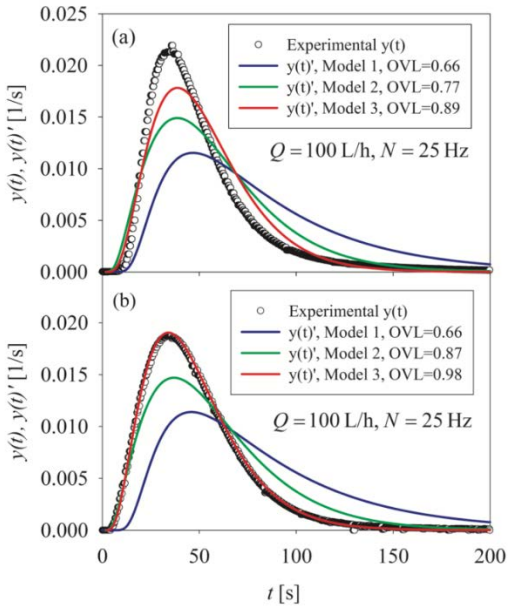

Fig. 9 Comparing the curve fitting of Model 1, Model 2 and Model 3.a: laminar flow with BREOX solution, Q_f=100 L/h, N=25 Hz; b turbulent flow with water, Q_f=100 L/h, N=25 Hz

5 Conclusions

For MBR using dynamic filtration module, RTD and thermal balance are an efficient way to diagnose bioprocess efficiency. In present work, a tracer injection and a detection method were applied to investigate RTD in an impeller-rotating filter (RVF module) in laminar and turbulent regimes.

Firstly, thermal effect was introduced in order to have the knowledge of temperature change and heat dissipation in a bioprocess context (cell culture).Thermal balance (heat dissipation) is correlated to mixing power (power consumption curve). The temperature increased dramatically at high rotation speed, especially in laminar flow (ex. +11°C under operating conditions Q_f=25 L/h and N=25 Hz). In turbulent flow, with Q_f =50 L/h and N=50 Hz, temperature increased up to 9°C. Considering a temperature increase limited to 4°C (compatible with cell culture), restricted operating conditions (minimum flowrate and maximum mixing rate) can be estimated from thermal balance and power consumption curve.

Secondly, experimental observation and analysis of RTD in this complex module are discussed. It has allowed the characterization of the flow behavior and the determination of defining parameter. Results indicated that in laminar flow, mean residence time ts remained constant at a given Q_f, whatever N was. Effective volume V1 was almost constant, slightly affected by flowrate, with a mean value at 1.3 L (87% out of the RVF total volume). In turbulent regime, t_s increased linearly as a function of N at a given Q_f. The effective volume V_1 was only mixing rate dependent, whereas flowrate had no effect. The effective volume ranged from 1.1 up to 1.6 L (74 up to 100% out of the RVF total volume). Combining with the CFD simulations in laminar regime (results were not shown in this article due to the limited pages), it indicated that a short-cut and dead-zone might exist in the RVF module. Modeling of RTD by PFR+(J) CSTR model (effective volume V1 and J=2.5±0.6) enabled to access to the mean residence time and its distribution for cells in a stressful environment.

Interactions between biological matrices and Dynamic Filtration must be deeply studied to intensify bioprocesses. Future works related to dynamic filtration may be focused on:, however, RTD of real process arise from a complex local interaction between the velocity profile, diffusion, turbulence, hear transfer, etc [10], studies might include:

- The investigation of local hydrodynamic [11] (velocity and shear stress profile etc.) to further prove mixing effect, and to better understand the flow pattern and coherent structure in the RVF module;
- The simulation of RTD with fluid streamlines, aim to verify the experimental results and gain insight for the flow streamlines.

Acknowledgements:
Financial support by China Scholarship Council is gratefully acknowledged (grant No. 201304490066). FR FERMAT has supported this work through experimental capacity. Authors wish to thank José Moreau and Bernard REBOUL (LISBP) for their mechanical contribution and Pascal DEBREYNE (PIHM, Lille) for data acquisition and electrical control for experimental setup.

Reference:

[1] Fillaudeau L., Boissier B., Ermolaev S., Jitariouk N., Gourdon A. Etude hydrodynamique d'un module de filtration dynamique. Revue des Industries Alimentaires & Agricole, Septembre / Octobre, 124 (9), (2007) 8-16.

[2] L. Fillaudeau, B. Boissier, A. Moreau, P. Blanpain-avet, S. Ermolaev, N. Jitariouk. Investigation of rotating and vibrating filtration for clarification of rough beer. Journal of Food Engineering. 80 (2007) 206–217. doi:10.1016/j.jfoodeng.2006.05.022.

[3] Y. El Rayess, Y. Manon, N. Jitariouk, C. Alabasi, M. Mietton Peuchot, A. Devatine and L. Fillaudeau. Wine clarification with Rotating and Vibrating Filtration (RVF): Investigation of the impact of membrane material, wine composition and operating conditions. Journal of Membrane Science, 513 (2016) 47–57, https://doi.org/10.1016/j.memsci.2016.03.058

[4] J. Villermaux. Génie de la réaction chimique: conception et fonctionnement des réacteurs. Ed

Technique Et Documentation. Paris, FR. ISBN 2852067595, (1999) 448p.

[5] J.H. Ham, B. Platzer, Semi-Empirical Equations for the Residence Time Distributions in Disperse Systems – Part 1: Continuous Phase, Chemical Engineering &Amp; Technology. 27 (2004) 1172–1178. doi:10.1002/ceat.200407038.

[6] D. Bošković, S. Loebbecke, G.A. Gross, J.M. Koehler, Residence Time Distribution Studies in Microfluidic Mixing Structures, Chemical Engineering &Amp; Technology. 34 (2011) 361–370. doi:10.1002/ceat.201000352.

[7] L.K. Wang, V. Ivanov, J.-H. Tay, eds. Environmental Biotechnology. Handbook of Environmental Engineering. Humana Press, Totowa, NJ, ISBN: 978-1-58829-166-0, 10 (2010) . doi:10.1007/978-1-60327-140-0.

[8] R.M. Walsh, P.A. Martin. Growth of Saccharomyces cerevisiae and Saccharomyces uvarum in a temperature gradient incubator. Journal of the Institute of Brewing. 83 (1977) 169–172. doi:10.1002/j.2050-0416.1977.tb06813.x.

[9] J. Thereska. L'application des radiotraceur dans les unités industrielles : bilan et perspectives ». Traceurs et Méthodes de Tracage. Recents Progres en Genie des Procedes (Ed. SFGP, Nancy, France), ISBN : 2-910239-37-7, 61 (12), (1998) 1-8.

[10] L. Fillaudeau, K. Le-Nguyen, C. André, Influence of flow regime and thermal power on residence time distribution in tubular Joule Effect Heaters, Journal of Food Engineering. 95 (2009) 489–498. doi:10.1016/j.jfoodeng.2009.06.010.

[11] X. XIE, C. Le Men, N. Dietrich, P. Schmitz, L. Fillaudeau, Local hydrodynamic investigation byPIV and CFD within a Dynamic filtration unit under laminar flow, Separation and Purification Technology. (in press 2017). doi:10.1016/j.seppur.2017